Taylor & Francis
Taylor & Francis Group

🔓 OPEN ACCESS   Check for updates

Unraveling ER dimerization dynamics in endocrine disruption based on a BRET-focused approach

Soomin Yum[a]*, Haksoo Lee[a]*, Yong-Kook Kwon[b], Gunyoung Lee[b], Hye-Young Lee[b], HyeSook Youn[c] and BuHyun Youn[a,d,e]

[a]Department of Integrated Biological Science, Pusan National University, Kumjeong-ku, Republic of Korea; [b]Food Safety Risk Assessment Division, National Institute of Food and Drug Safety Evaluation, Cheongju-si, Republic of Korea; [c]Department of Integrative Bioscience and Biotechnology, Sejong University, Seoul, Republic of Korea; [d]Department of Biological Sciences, Pusan National University, Busan, Republic of Korea; [e]Nuclear Science Research Institute, Pusan National University, Busan, Republic of Korea

ABSTRACT

Endocrine-disrupting chemicals (EDCs) are exogenous compounds that interact with the estrogen receptor (ER), thereby disrupting estrogen-mediated signaling. In a previous study, we employed a bioluminescence resonance energy transfer (BRET) system to assess ER dimerization for detecting EDCs. To further determine whether the BRET assay could be used independently to identify EDCs, we investigated ER-EDC interactions before and after dimerization. Results from isothermal titration calorimetry (ITC) and dynamic light scattering (DLS) revealed that ER dimerization can be mediated by EDCs. Consequently, the BRET assay proved effective in detecting dimerization and clarifying its relevance to EDC-induced signaling disruption. Additionally, to examine EDC-induced transcriptional changes, we performed chromatin immunoprecipitation sequencing (ChIP-seq), followed by gene ontology (GO) analysis. These analyses demonstrated that EDCs affect various signaling pathways, including those involved in antibody-dependent cytotoxicity, bone morphogenetic protein (BMP) signaling in cardiac induction, and hepatocyte growth factor receptor signaling. Overall, this study elucidates the molecular mechanisms by which EDCs influence ER dimerization and signaling. These findings highlight the utility of the BRET-based assay for EDC detection and contribute to a deeper understanding of the systemic effects of EDCs on endocrine disruption.
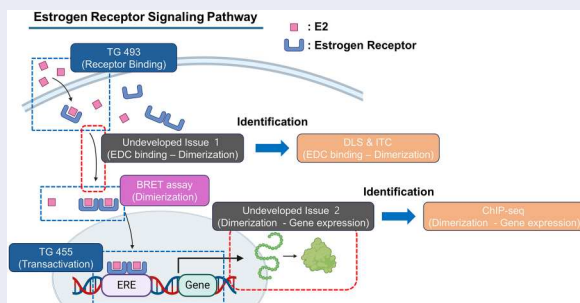
Introduction

Endocrine-disrupting chemicals (EDCs) have emerged as significant environmental and public health concern (Zoeller et al. 2012; Moon et al. 2023). EDCs are pervasive in modern life, found in common items like plastic food containers and water bottles, pesticides applied to crops, and ingredients in personal care products.

Humans are primarily exposed to EDCs through ingestion (contaminated food and water), inhalation (breathing dust or vapors containing EDC), and dermal absorption (direct skin contact with EDC-containing materials) (Antony et al. 2022, Park, Jang, et al. 2024). EDCs can interfere with hormone signaling in organisms, affecting processes such as metabolism, immunity, and

development (Park, Lee, et al. 2024; Yilmaz et al. 2020). Among these, estrogenic EDCs (eEDCs) disrupt estrogen signaling. By mimicking or inhibiting the natural hormone 17β-estradiol (E2), eEDCs can disturb normal endocrine functions, potentially contributing to reproductive disorders, developmental abnormalities, and other adverse outcomes (Diamanti-Kandarakis et al. 2009; Rachoń 2015; Dutta et al. 2023; Huang et al. 2023).

Estrogen signaling through the estrogen receptor (ER) involves three sequential steps: (1) binding of E2 to the ER, (2) receptor dimerization, and (3) binding of the resulting ER dimer to estrogen response elements (EREs) on target genes (Welboren et al. 2009; Liang and Shang 2013). Standardized test guidelines established by the Organization for Economic Cooperation and Development (OECD), such as test guideline (TG) 493 for ligand binding assessment (OECD TG 493) and TG 455 for ERE-mediated transcriptional activation (OECD TG 455), have facilitated robust assessments of these processes (OECD 2021, OECD 2024). TG 493 examines ligand binding using radiolabeled assays, whereas TG 455 measures ERE-mediated transcriptional activation through a luciferase reporter system. These methods effectively evaluate the first and third steps of the ER signaling pathway (Kim et al. 2011). However, the second step, ER dimerization, remains insufficiently addressed by current standardized approaches. The importance of assessing ER dimerization is particularly evident when certain chemicals, such as testosterone, yield contradictory outcomes in existing assays (ICCVAM 2003). For instance, testosterone may bind to the ER (as indicated by TG 493), yet fails to induce downstream transcriptional responses in TG 455. Such discrepancies suggest that EDCs can selectively alter the intermediate steps of ER signaling, potentially through non-canonical binding sites, alternative signaling partners, or other regulatory mechanisms (Leclercq et al. 2011; Souza et al. 2019). Our understanding of these intermediate disruptions remains incomplete without a dedicated assay for assessing ER dimerization. Furthermore, a comprehensive analysis of the pre- and post-dimerization steps is essential to elucidate this integrated mechanism. Additional studies are needed to investigate how dimerization dynamics vary with ligand binding and how gene expression is modulated by the extent of dimerization. Understanding these integrative processes will provide critical validation for using dimerization as an independent measure of EDCs.

To address this gap, we previously developed a bioluminescence resonance energy transfer (BRET) assay specifically designed to detect and quantify ER dimerization events (Choi et al. 2024). While this new tool provides a crucial component in the evaluation of ER signaling, it needs to be integrated into a broader testing framework. The interactions between ligand binding, ER dimerization, and subsequent transcriptional activation, are complex (Tamrazi et al. 2002). A comprehensive approach that links these steps would enable more reliable detection and risk assessment of EDCs.

In the present study, we employed a BRET-based assay to examine ER dimerization in the presence of candidate EDCs. These measurements were complemented by dynamic light scattering (DLS) (Gast and Fiedler 2012) and isothermal titration calorimetry (ITC) (Freyer and Lewis 2008) to verify binding affinities and receptor complex formation. Additionally, we performed chromatin immunoprecipitation sequencing (ChIP-seq) (Nakato and Sakata 2021) to determine how EDC-induced perturbations in ER dimerization translate into changes in gene expression. By correlating disruptions in ER dimerization with alterations in target gene networks, our study not only elucidates the molecular mechanisms of endocrine disruption but also highlights the critical role of dimerization. Through this integrated strategy, we established a more accurate framework for EDC detection, aiding in the development of more predictive and reliable assessment methods, and enhancing our fundamental understanding of ER-mediated signaling pathways.

Materials and methods

Cell culture

MCF-7 (Korea Cell Line Bank, 30022) cells were cultured in Dulbecco's modified Eagle's medium (DMEM; Welgene, LM 001-05) supplemented with 10% fetal bovine serum (FBS; Gibco, 16000-044) and 100 U/ml penicillin alongside 100 μg/ml streptomycin (GenDepot, CA005). Cultured cells were maintained in an incubator with 5% CO_2 at 37 °C.

BRET assay

This method was used in previous study. To optimize the acceptor and linker, ERα/β BRET biosensors were transfected into HEK-293 T cells. After 24–36 hours of transfection, cells were harvested and resuspended in assay media. A total of 100,000 cells were seeded into white-bottom 96-well plates (SPL, 30196) and incubated overnight. E2 was subsequently added to the wells to achieve a final concentration of 1 μM. After 24 hours of treatment, NanoBRET Nano-Glo Substrate (final dilution 1:200) was injected into the wells 15 minutes prior to luminescence measurement. Luminescence signals were recorded using a CLARIOStar Plus microplate reader (BMG Labtech) at 37°C. Signals were measured

at wavelengths of 450 ± 40 nm (NLuc intensity), 650 ± 50 nm (HaloTag BRET intensity), and 640 ± 50 nm (Cyofp1 BRET intensity).

For the EA screening assay, the assay media consisted of clear DMEM (Welgene, LM001-17) supplemented with 0.5% FBS, 1% penicillin (100 U/mL), and 1% streptomycin (100 μg/mL). Stable cell lines were cultured in 75 T flasks (SPL, 70075) and harvested prior to initiating the assay. Cells were resuspended in assay media, and 50,000 cells were plated into white solid-bottom 96-well half-area plates (Greiner Bio-One, 675083), followed by overnight incubation. The Endurazine substrate (final dilution 1:100) was added to the wells 2 hours prior to luminescence measurement. Baseline luminescence data were recorded, and the cells were subsequently treated with E2 and EAs at a final concentration of 1 μM. Luminescence was measured at 6, 12, and 24 hours post-treatment using a CLARIOStar Plus microplate reader at 37 °C. The filter set used for luminescence detection included 460 ± 40 nm (NLuc intensity) and 615 ± 20 nm (BRET intensity).

Dose–response curves (sDRCs) and logEC values were generated using the built-in 'log(agonist) vs. response-variable slope' equation in GraphPad Prism 9. EC10nBR, EC50nBR, EC90nBR, and EAnBR values were calculated accordingly. The BRET ratio and normalized BRET signals (nBR) were determined using the following formulas.

Plasmid construction, expression and purification

Expression plasmids, pET28a-ERα-LBD and pET28a-ERβ-LBD were constructed using a polymerase chain reaction strategy. A specific region of human ERα-LBD (aa304-aa554) and ERβ-LBD (aa264-aa498) were amplified by polymerase chain reaction using the cDNA clone as a template. A sense primer ERα-LBD-F (5'- ACGTCAGGATC-CATGAACAGCCTG -3') and ERβ-LBD-F (5'- TGCAGTG-GATCCATGAGCCCCGAG -3') that contain a BamHI site and a start codon, respectively, and an antisense primer ERα-LBD-B (5'- ACGTCACTCGAGGCGCCCACTAGC -3') and ERβ-LBD-B (5'- ACGTCACTCGAGCTGAATGCCCAC -3') that contain a XhoI site, respectively, were used for ERα-LBD or ERβ-LBD construct.

ERα-LBD or ERβ-LBD expression was carried out by inoculating 100 ml of LB supplemented with 30 μg/ml kanamycin from a freezer stock of pET28a-ERα-LBD or pET28a-ERβ-LBD in BL21(DE3) cells. This was allowed to grow overnight at 37 °C with constant shaking, after which this culture was used to inoculate 1.5 liters of LB medium. Protein expression was induced by addition of isopropyl β-D-thiogalactopyranoside to a final concentration of 0.5 mM at mid-log phase growth (A600

= ∼0.6). Following induction, the cells were incubated at 20 °C for 12 h with shaking at 250 rpm. Cells were harvested by centrifugation at 3,000 × g, and pellets were frozen to promote lysis. The cell pellet was then thawed at room temperature, resuspended in a minimal volume of lysis buffer (50 mM Tris (pH 8.0), 300 mM NaCl, and 20 mM imidazole for TftC, 20 mM Tris (pH 8.5)), sonicated 10 times for 10 s each using a model 450 Sonifier®(Branson Ultrasonics), and the resulting lysate cleared by centrifugation (20,000 × g for 40 min).

For the ERα-LBD or ERβ-LBD purification, the lysate was applied to a nickel-nitrilotriacetate column and washed with several column volumes of lysis buffer. Elution took place with the lysis buffer containing 300 mM imidazole. Eluted fractions containing ERα-LBD or ERβ-LBD were combined, concentrated, and buffer-exchanged into 20 mM Tris (pH 8.5) containing 50 mM NaCl by ultrafiltration in an Amicon 8050 cell with a 30-kDa cutoff membrane (Millipore). ERα-LBD or ERβ-LBD was then applied to an ion-exchange column (Bio-Rad Uno Q12), and the protein of interest was collected in the flowthrough. ERα-LBD or ERβ-LBD was then concentrated and added to several volumes of 5 mM sodium phosphate (pH 6.8). Precipitates formed during this step were removed by centrifugation, after which the remaining solution, containing only ERα-LBD or ERβ-LBD was concentrated and exchanged into 20 mM Tris (pH 7.5). With the exception of the nickel-nitrilotriacetate column, all purification steps were carried out using an Amersham Biosciences/BioCad 700E preparative HPLC (Applied Biosystems). All purification steps were monitored, and final homogeneity (>99%) was estimated using SDS-PAGE and Coomassie Blue staining.

Dynamic light scattering

To test for the formation of multimeric status of ERα-LBD or ERβ-LBD, we used a DynaPro Titan (Wyatt Technology Corp.). A scan was taken of each protein individually as well as a scan containing a 17β-estradiol (1 μM) or zwitterionic detergent, CHAPS, was added just before each experiment. Measurements consisted of 10 consecutive 5-s scans, and average molecular radius was measured using a Rayleigh sphere approximation. Data were analyzed using the manufacturer- supplied software, Dynamics 6.7.3.

Isothermal titration calorimetry

The heats of binding of ERα-LBD or ERβ-LBD with various EDCs were measured with a VP-ITC Microcalorimeter (Microcal, Northampton, MA). For calorimetric

measurements, ERα-LBD or ERβ-LBD in 20 mM Mops (pH 7.2), 100 mM NaCl, 1 mM dithiothreitol was titrated with one of the EDCs dissolved in the same buffer. The apo-form ERα-LBD, ERβ-LBD and EDC solutions were degassed prior to titration. The experiment consisted of 29 injections of 10 µl each of ligand into the protein solution at 25 °C with constant stirring at 300 rpm employing a 300-s equilibration interval between injections. Heats of dilution of each ligand were determined by titration of the ligand into buffer without protein and were used to correct the protein titration data.

Data were fit to an n-equivalent binding sites model at first by nonlinear least-squares regression with the Origin software package (OriginLab Corp, Northampton, MA). Because the number of binding.

sites (n) was converged to values between 0.8 and 1.2 by the initial regressions, it was fixed to 1.0 (one binding site model) in the final regressions. The fit of data yields the binding affinity, enthalpy change, entropy change, and binding stoichiometry for the titration. EDCs with positive interactions with ERα-LBD or ERβ-LBD were subjected to repeat experiments, and affinities for the interactions were determined by averaging results across experiments. Other EDC that did not show significant heats of reaction were not subjected to repeat experiments. The EDCs that were screened for interaction with ERα-LBD or ERβ-LBD were 5α-Dihydrotestosterone, 17α-estradiol, 17β-estradiol, Bisphenol B, Diethylstilbestrol, Estrone, 4-tert-Octylphenol and flutamide. All compounds were purchased from Sigma-Aldrich.

RNA extraction and qRT-PCR

Total RNA was extracted with AccuPrep® Universal RNA Extraction Kit (#K-3140, Bioneer, Korea). Synthesize cDNA was analyzed by Real-time qRT-PCR using an Applied Biosystems StepOne Real-Time PCR System (Applied Biosystems, USA). The qPCR primers are listed in Supplementary Table 1. Each sample was assessed by triplication.

Chromatin immunoprecipitation (ChIP)

This study utilized the Pierce Magnetic ChIP Kit (Thermo, 26157), and the method was as follows:

The estrogen α antibody, ab32063 (Abcam), estrogen β antibody GTX70174 (GeneTax) were used for ChIP. Cells were cultured, treated as required, and crosslinked by adding formaldehyde (1% final concentration) for 10 min at room temperature. Glycine (1X) was added to quench crosslinking for 5 min. Cells were washed with PBS, scraped in PBS containing Halt Cocktail, and pelleted by centrifugation at 3000 × g for 5 min. Pellets

were resuspended in Membrane Extraction Buffer with inhibitors, vortexed briefly, and incubated on ice for 10 min. Nuclei were isolated by centrifugation at 9000 × g for 3 min, resuspended in MNase Digestion Buffer, and digested with 2 µL of diluted MNase (1:10) per $4 × 10^6$ cells at 37 °C for 15 min. The reaction was stopped, and nuclei were pelleted, resuspended in IP Dilution Buffer, and sonicated (3 × 20 s pulses). Lysates were centrifuged at 9000 × g for 5 min, and the supernatant containing chromatin was collected. Chromatin was diluted in IP Dilution Buffer and incubated with antibodies (e.g. anti-RNA Pol II or target-specific) at 4 °C for 2 h to overnight. After overnight, protein A/G Magnetic Beads were added and incubated for 2 h. Beads were washed three times with Wash Buffer 1 and once with Wash Buffer 2. Chromatin was eluted with IP Elution Buffer at 65 °C for 30 min and treated with NaCl and Proteinase K at 65 °C for 1.5 h to reverse crosslinks. DNA was purified using a DNA Clean-Up Column and eluted in Elution Solution for downstream applications.

Results

A BRET assay detects EDCs by targeting ER dimerization

EDCs interfere with the endocrine system by targeting the ER signaling pathway, making accurate detection and characterization essential (Yoon et al. 2014). Current standardized methods for EDC detection include TG 493, which evaluates ER ligand binding, and TG 455, which assesses estrogen response element (ERE) transactivation using luciferase reporter assays (Figure 1A). However, discrepancies arise when compounds bind to ERs but do not trigger ERE-mediated activity, suggesting other mechanisms beyond standard ER dimerization. This context highlights the need for methods capable of detecting dimerization to overcome existing limitations. In particular, two aspects remain under investigated: EDC binding–dimerization (Figure 1A, Undeveloped Issue 1) and dimerization–gene expression (Figure 1A, Undeveloped Issue 2). Although existing guidelines address ligand binding and transcriptional activation, further research is needed to bridge these intermediate steps. Our study aims to clarify and expand upon these underexplored areas.

To address the gap of binding-dimerization and dimerization-transactivation, we developed a BRET assay and established cell lines expressing ERα-α, ERα-β, and ERβ-β dimers (Figure 1B). The BRET assay measures ER subtype dimerization after treatment with estrogenic ligands, such as E2, by detecting changes in the BRET ratio. This method enables the identification
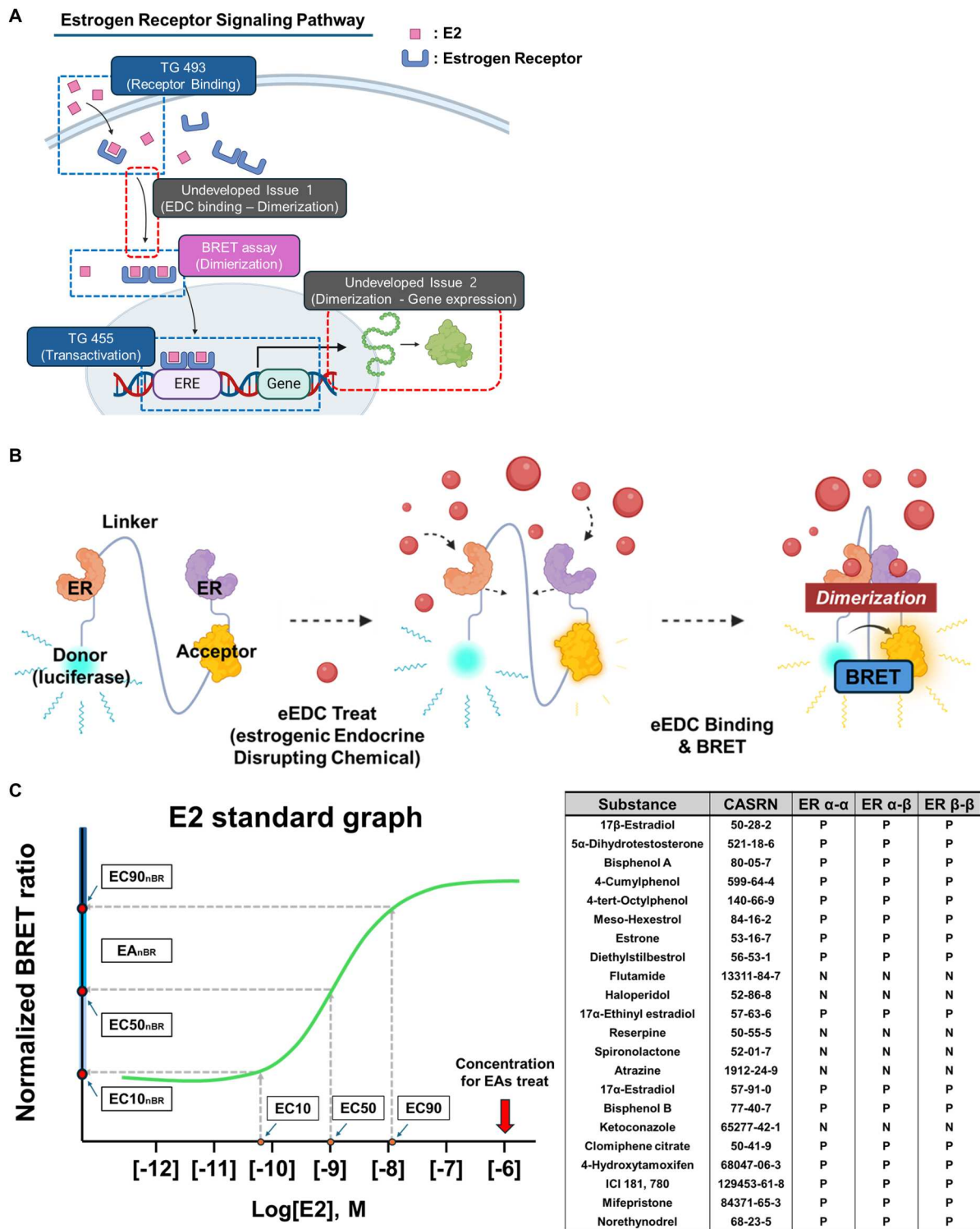
Substance	CASRN	ER α-α	ER α-β	ER β-β
17β-Estradiol	50-28-2	P	P	P
5α-Dihydrotestosterone	521-18-6	P	P	P
Bisphenol A	80-05-7	P	P	P
4-Cumylphenol	599-64-4	P	P	P
4-tert-Octylphenol	140-66-9	P	P	P
Meso-Hexestrol	84-16-2	P	P	P
Estrone	53-16-7	P	P	P
Diethylstilbestrol	56-53-1	P	P	P
Flutamide	13311-84-7	N	N	N
Haloperidol	52-86-8	N	N	N
17α-Ethinyl estradiol	57-63-6	P	P	P
Reserpine	50-55-5	N	N	N
Spironolactone	52-01-7	N	N	N
Atrazine	1912-24-9	N	N	N
17α-Estradiol	57-91-0	P	P	P
Bisphenol B	77-40-7	P	P	P
Ketoconazole	65277-42-1	N	N	N
Clomiphene citrate	50-41-9	P	P	P
4-Hydroxytamoxifen	68047-06-3	P	P	P
ICI 181, 780	129453-61-8	P	P	P
Mifepristone	84371-65-3	P	P	P
Norethynodrel	68-23-5	P	P	P

Figure 1. EDCs act through the estrogen signaling pathway, and can be screened by confirming dimerization via BRET. (A) Schematic representation of the estrogen receptor signaling pathway, illustrating how EDC testing compounds are evaluated using TG 455, TG 493, and the BRET assay, which assesses dimerization. TG 455 and TG 493 (blue), along with the BRET assay (pink) are positioned at their respective stages within the ER signaling pathway. Gray boxes highlight the areas where assay development remains limited. (B) Schematic illustration of the predicted mechanism underlying the BRET assay. (C) Schematic depiction of the calculation process: First, a standard curve for E2 was generated by serially diluting E2 tenfold (solid green line). From this curve, EC10, EC50, and EC90 values were converted to normalized BRET ratio (nBR) values. Next, the EC values were located on the X-axis (orange filled circles), and their corresponding nBR values (red filled circles) were determined by following the dashed lines (gray dashed arrows) to the Y-axis. Finally, EC_{nBR} and EA_{nBR} values were compared to classify EAs (all treated at 1 µM) into distinct groups. Using this criterion, we identified 16 EDCs with $EC50_{nBR}$ values above the $EC50_{nBR}$ value for both ER α-α, α-β, and β-β (represented by P) and 6 EDCs with $EC50_{nBR}$ values below the $EC50_{nBR}$ value (represented by N).

of EDCs based on how they affect ER dimerization. We determined baseline BRET ratios using various E2 concentrations, which allowed define effective concentration (EC)10, EC50, and EC90 values. EDCs were then identified by deviations in the BRET ratio, providing a sensitive and rapid method to detect ER dimerization. Based on the BRET assay results, we identified 16 compounds exhibiting a positive BRET ratio and 6 compounds showing a negative BRET ratio across ERα-α, ERα-β, and ERβ-β dimers. These selected compounds were subsequently used in the following experiments (Figure 1C).

While the BRET assay is effective for monitoring ER dimerization, further research is needed to clearly understand how EDCs, ER binding, and subsequent steps in the signaling pathway interact. Important factors that warrant further study include EDC binding affinities and how this affects dimerization and downstream signaling events. The findings of this study highlight the potential of the BRET assay to enhance existing EDC detection methods and improve our understanding of the underlying mechanisms.

DLS analyses reveal E2-stabilizes ER-LBD dimerization

We utilized DLS to investigate how EDCs affect the dimerization of the ligand-binding domains (LBDs) of ERα and ERβ, which are the primary binding sites for EDCs. DLS measures the hydrodynamic radius of particles in solution by analyzing the fluctuations in scattered light intensity. Larger particles diffuse more slowly, resulting in slower fluctuations, while smaller particles diffuse more rapidly, resulting in faster fluctuations. This technique provides insights into the size distribution of particles within a sample. In the context of ER dimerization, if EDCs promote or stabilize the formation of ER dimers, we would anticipate an increase in the average particle size measured by DLS, which would be indicated by a shift toward larger hydrodynamic radii. The LBDs of ERα (residues 947–1680) and ERβ (residues 790–1506) have predicted molecular weights of 28 and 27 kDa, respectively (Figure 2A) (Min et al. 2021). We conducted DLS under three different conditions: (1) with detergent, (2) without detergent, and (3) without detergent but with E2 (1 μM). For the detergent-treated samples, we used CHAPS (3-((3-cholamidopropyl)dimethylammonio)-1-propanesulfonate, 0.5% w/v) (Herrera et al. 2014), an amphoteric detergent that breaks non-covalent interactions while preserving protein structure. It has been reported that ER can form dimers even in the absence of a ligand; however, these dimers are generally less stable, exhibiting a

higher dissociation rate (Tamrazi et al. 2002). Our DLS data indicated that, in the absence of detergent, both ERα- and ERβ-LBDs primarily exhibited dimeric peaks, alongside occasional monomeric peaks. Upon adding E2, the DLS profile showed a single dimeric peak with a predicted molecular radius of approximately 3.18 nm and a molecular weight of around 60 kDa, closely aligning with the expected molecular weight of the ER-LBD dimer in 2 mg/mL buffer solution. However, the addition of detergent treatment disrupted dimerization, resulting in a monomeric peak with a predicted radius of 1.75 nm and an approximate molecular weight of 30 kDa (Figure 2B and C).

Collectively, the E2-treated samples exhibited only dimeric peaks, with no detectable monomers, indicating that E2 stabilizes the dimeric state. These results suggest that while ER dimerization can occur in the absence of a ligand, ligand binding significantly enhances and stabilizes the dimer. This stabilization likely facilitates the receptor's translocation into the nucleus and subsequent transcriptional regulation, underscoring the crucial role of ligand binding in preserving the dimeric structure and functionality of the ER.

ITC-measured EDC-ER affinities validate dimerization detected by BRET

To investigate the variation in BRET ratios observed for different EDCs in our previous experiments, we first assessed the binding affinities of selected EDCs to the ER LBDs. We employed isothermal titration calorimetry (ITC), a powerful biophysical technique that directly measures the thermal changes associated with biomolecular binding interactions. In ITC, a solution of the ligand (in this case, EDC) is titrated into a sample cell containing the target macromolecule (ER LBD), while the heat released or absorbed during the binding process is carefully monitored. The resulting titration curve can be analyzed to determine the binding affinity (K_d), stoichiometry (n), enthalpy change (ΔH), and entropy change (ΔS) for the interaction. From the 22 EDCs previously tested with the BRET system (Choi et al. 2024), we selected eight – E2, diethylstilbestrol, 4-tert-octylphenol, estrone, 17α-estradiol, 5α-dihydrotestosterone, bisphenol B, and flutamide – based on their impact on the BRET ratio. This selection allowed us to focus on EDCs that are most likely to demonstrate significant differences in binding behavior.

We then conducted ITC experiments to measure the binding affinities of these EDCs to ERα- and ERβ-LBDs. Among the compounds tested, diethylstilbestrol exhibited the highest binding affinity to ERα-LBD at 0.8 μM, followed by E2 at 2.2 μM, 17α-estradiol at 3.4 μM,
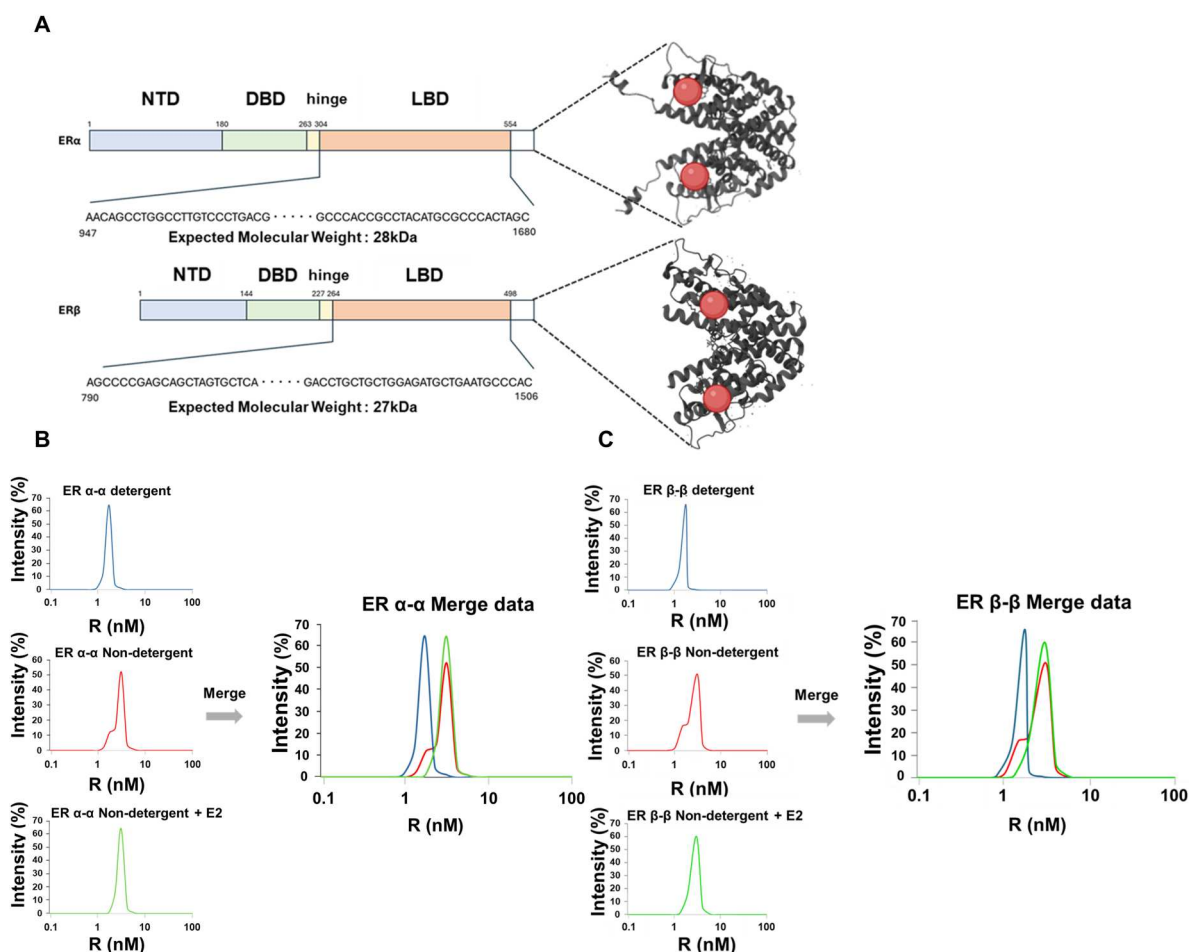
A

B

C

Figure 2. ER dimerization occurs independently of ligand binding. (A) The domain structures of ERα and ERβ are presented. Among these domains, the ligand-binding domain (LBD) of ERα spans 733 amino acids with an expected molecular weight of 28 kDa, while the LBD of ERβ consists of 716 amino acids with an expected molecular weight of 27 kDa. (B and C) Dynamic light scattering (DLS) profiles of ERα-α and ERβ-β are shown. The intensity distributions corresponding to hydrodynamic radius (R) were measured under three conditions: in the presence of the detergent CHAPS (blue line), after treatment with E2 (green line), and without any treatment (red line). Both the CHAPS-treated and E2-treated samples exhibited a single distinct peak, whereas the untreated samples showed two separate peaks, indicating that ligand binding further stabilizes, but does not solely initiate, ER dimerization.

estrone at 10.6 µM, 4-tert-octylphenol at 33.4 µM, bisphenol B at 112.0 µM, and 5α-dihydrotestosterone at 152.0 µM. A similar pattern was observed for the ERβ-LBD, with diethylstilbestrol again showing the highest affinity at 0.9 µM, followed by E2 at 1.8 µM, 17α-estradiol at 12.8 µM, 4-tert-octylphenol at 15.9 µM, estrone at 30.9 µM, bisphenol B at 51.3 µM, and 5α-dihydrotestosterone at 152.0 µM. In contrast, flutamide exhibited no binding to either ER subtype (Figure 3A, B, and Supplementary Table 2).

These findings align with the previous data on EDC binding to ERα and ERβ, revealing a consistent pattern: compounds with higher binding affinities tend to induce greater changes in ER dimerization, as indicated by the BRET ratios. This correlation between binding affinity and dimerization confirms that the utility of BRET system in identifying EDCs and understanding

their impact on ER dimer formation. Notably, the observed trends for both ER subtypes suggest that this method can effectively distinguish how different EDCs interact with ERα and ERβ. Collectively, these results highlight the significance of ER dimerization in EDC-affected signaling and highlight the necessity of monitoring this step for more accurate detection and understanding of EDCs.

EDC-induced ER dimerization correlates with gene expression driven by ERE

We observed that ER dimerization occurred even in the absence of EDCs; however, the binding affinity of the EDCs influenced both the recruitment and stabilization of these dimers. Given that nuclear translocation and transcriptional activation occur downstream of
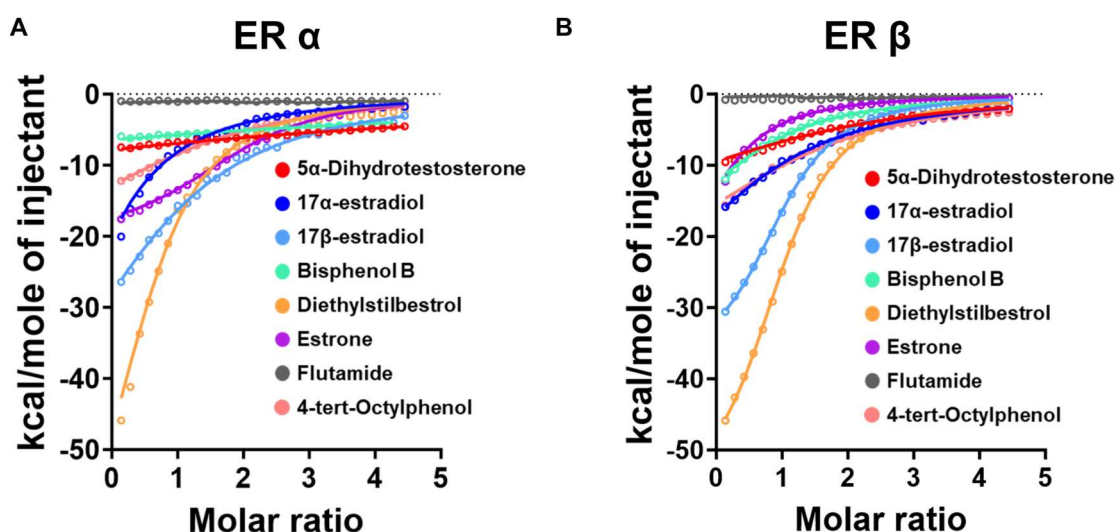
Figure 3. Different EDCs exhibit varying binding affinities, reflected in distinct BRET ratios. (A and B) Isothermal titration calorimetry (ITC) profiles for ERα–α and ERβ–β dimers were analyzed with eight EDCs: 5α-dihydrotestosterone, 17α-estradiol, 17β-estradiol, bisphenol B, diethylstilbestrol, estrone, flutamide, and 4-tert-octylphenol. The graphs display the enthalpy change (kcal/mol) as a function of the molar ratio of ligand to receptor, illustrating how each compound's binding affinity correlates with its effect on ER dimerization. The X-axis represents the molar ratio of ligand to receptor, where a molar ratio of 1 indicates that the total moles of injected ligand equal the moles of receptor present in the cell.

dimerization, we employed the BRET assay to correlate the extent of dimerization with alterations in gene expression (Han et al. 2024). To explore how varying levels of dimerization affect gene expression, we focused on ERE-mediated transactivation. We measured luminescence intensity at the ERE binding site following treatment with the 22 EDCs previously identified by the BRET assay. A diverse range of luminescence intensities was observed (Figure 4A), reflecting the different effects of each EDC on ERE transactivation. Subsequently, we assessed whether these changes in ERE transactivation impacted gene expression. For this purpose, we selected four well-known E2-related genes – cathepsin D (Perkins et al. 2022), progesterone receptor, the gene regulated by estrogen in breast cancer 1 (GREB1) (Cheng et al. 2018), and Bcl-2 (Marie et al. 2023) – to serve as representative targets.

Promoter analysis of these genes revealed that EREs act as critical regulatory sites for ER-mediated transcription, with variations in the number and positioning of EREs among different genes (Figure 4B). We subsequently examined the changes in gene expression induced by the 22 EDCs, including E2. Based on prior BRET assay results, we established optimal treatment conditions (1 μM E2 for 36 hours) through dose–response and time-course experiments (Figure 4C and D). Under these conditions, cells were treated with the selected EDCs, and gene expression was analyzed (Figure 4E). The results indicated that ERE transcriptional activity was closely related to the EDC-induced changes

in gene expression, reflecting either increases or decreases. This demonstrates a direct relationship between ERE-driven transcription and the alterations in gene expression induced by EDCs. Collectively, these findings provide critical insights into the molecular mechanisms underlying EDC-mediated endocrine disruption, directly addressing the issues outlined in Figure 1A (Undeveloped Issue 2) by demonstrating how ER dimerization translates into changes in gene expression. Moreover, they emphasize the utility of the BRET assay for characterizing EDC-induced transcriptional changes, thereby advancing our understanding of the mechanisms underlying endocrine disruption.

ChIP-seq and Gene Ontology (GO) analysis reveal EDC-driven transcriptional shifts and ERE-linked biomarkers

Analysis of the ERE sequences in the promoter regions of the four selected genes revealed differences in both the location and number of EREs. Nonetheless, the observed gene expression changes closely aligned with the results of the ERE transactivation assay. To expand our understanding beyond individual genes, we performed ChIP-seq to evaluate global gene expression changes (Figure 5A). For these analyses, we selected three EDCs that resulted in positive BRET ratios—5α-dihydrotestosterone, 17α-estradiol, and bisphenol B – as well as one EDC with a negative BRET ratio, flutamide. Flutamide acts as a competitive antagonist of the androgen
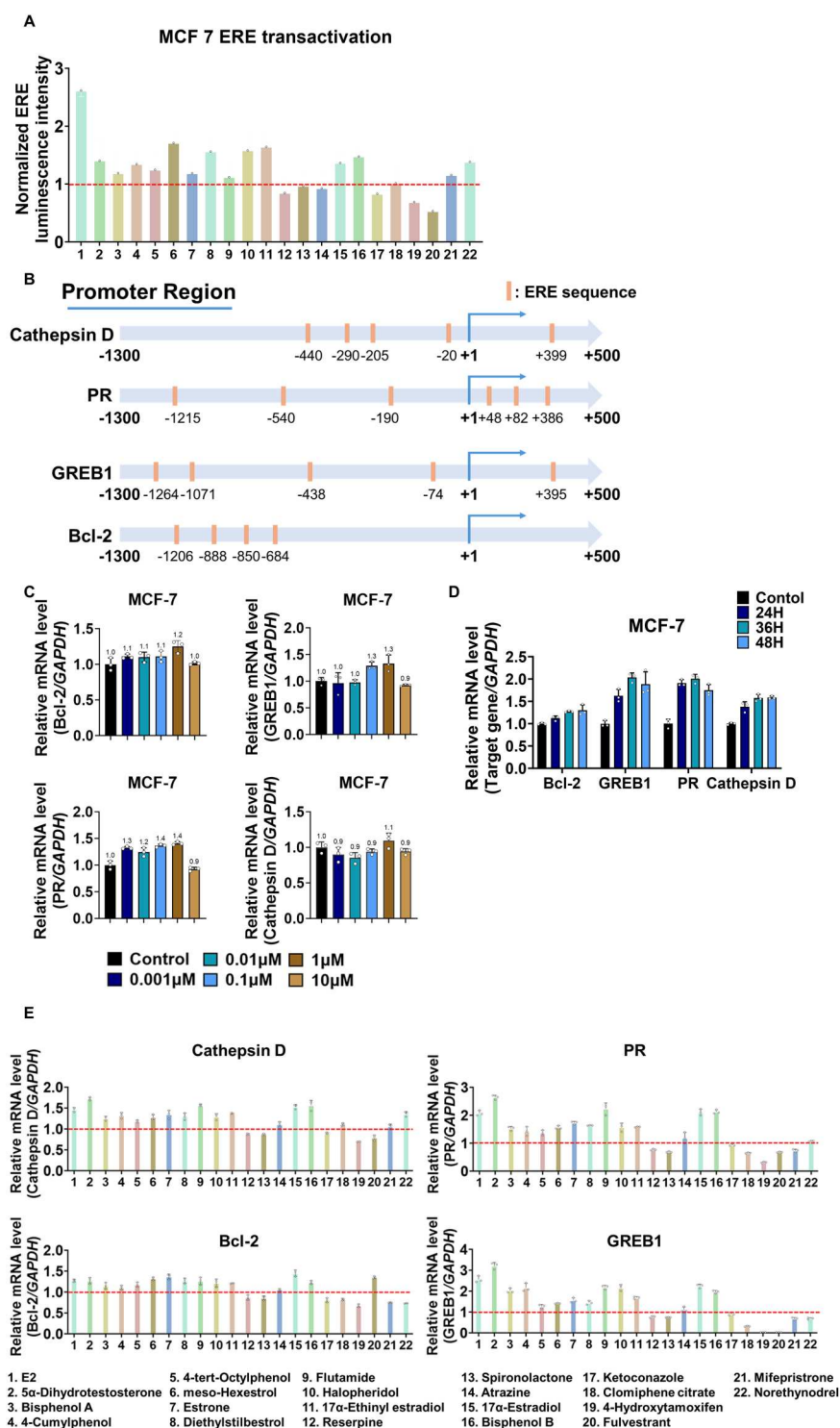
Figure 4. E2-related gene expression varies with ERE transactivation. (A) The diagram illustrates the ERE sequences within the promoter regions of four genes: Cathepsin D, Progesterone Receptor (PR), GREB1, and Bcl-2. (B) To determine the optimal treatment concentration, MCF-7 cells were treated with various concentrations of E2 (0.001, 0.01, 0.1, 1, and 10 μM), alongside a DMSO control. Gene expression changes were then assessed. (C) To identify the optimal treatment duration, MCF-7 cells were treated with E2 for 24, 36, and 48 hours, with a DMSO control. Gene expression changes were subsequently measured. (D) Following treatment with 22 selected EDCs (1 μM, 36 hours), mRNA levels of Cathepsin D, PR, GREB1, and Bcl-2 were evaluated. The bar graphs display expression levels normalized to the DMSO control (red line) for each EDC treatment. (E) ERE transactivation was measured in response to the same 22 EDCs, with all values normalized to the DMSO control (red line). This allowed for the quantification of how each EDC influenced ERE-driven transcription.
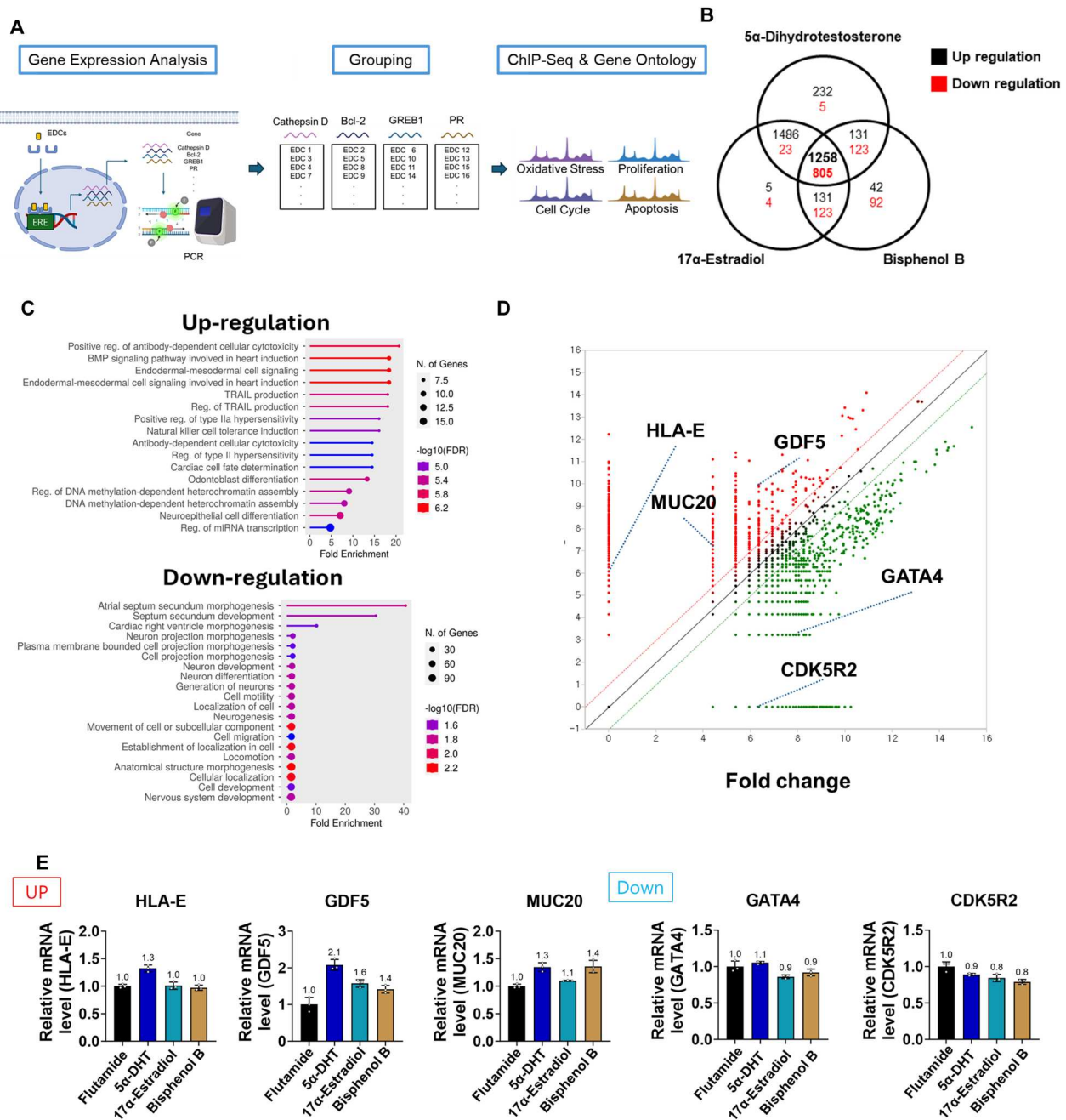
Figure 5. ChIP-seq reveals EDC-driven gene regulation mediated by ERα and ERβ. (A) Schematic overview of the ChIP-seq experiment utilizing ERα and ERβ antibodies. (B) Venn diagram comparing three EDCs with positive BRET ratios (5α-dihydrotestosterone, 17α-estradiol, and bisphenol B) against flutamide (negative BRET ratio). A total of 1,258 genes were upregulated and 805 were downregulated by these three EDCs compared to flutamide. (C) Gene Ontology (GO) analysis following treatment with four EDCs—5α-dihydrotestosterone, 17α-estradiol, bisphenol B, and flutamide—shows significant changes relative to flutamide alone. Key enriched pathways include antibody-dependent cellular cytotoxicity (ADCC), BMP signaling in cardiac development, and the hepatocyte growth factor receptor signaling pathway. (D) Scatter plot analysis identifies genes associated with the enriched GO terms. HLA-E is upregulated in ADCC, GDF5 is linked to BMP signaling in cardiac induction, and MUC20 is involved in the hepatocyte growth factor receptor signaling pathway. (E) Relative mRNA expression of EDC-related genes in MCF-7 cells treated with flutamide, 5α-dihydrotestosterone, 17α-estradiol, or bisphenol B (1 μM) is presented. HLA-E, GDF5, and MUC20 are upregulated, whereas GATA4 and CDK5R2 are downregulated, consistent with the ChIP-seq findings.

receptor (AR) and is not classified as an estrogen. It has demonstrated no activity in previous TG 455 and BRET assay. Therefore, making it an appropriate negative control for ChIP-seq analysis (Zacharia 2017).

Comparative analysis revealed that 1,258 genes were upregulated and 805 were downregulated in cells treated with the three BRET-positive, estrogen-like EDCs, compared to flutamide-treated cells (Figure 5B).

GO analysis of these differentially expressed genes identified significant biological processes affected by EDC treatment. Notably, we observed enrichment of processes related to the positive regulation of antibody-dependent cellular cytotoxicity, the BMP signaling pathway involved in cardiac induction, and the hepatocyte growth factor receptor signaling pathway for 5α-dihydrotestosterone, 17α-estradiol, and bisphenol B, respectively (Figure 5C).

Further examination of the enriched GO terms indicated that EDC exposure modulated a variety of biological processes, including immune-related pathways (e.g. inflammatory responses) as well as signaling and growth pathways in hepatocytes and cardiac cells. Scatter plot analyses revealed notable increases in HLA-E (associated with antibody-dependent cytotoxicity) (Rölle et al. 2018), GDF5 (linked to BMP signaling in cardiac induction) (Sorsby et al. 2024), and MUC20 (related to hepatocyte growth factor receptor signaling) (Higuchi et al. 2004). Conversely, we observed significant decreases in GATA4 (involved in atrial septum secundum morphogenesis) (Nadeau et al. 2010) and CDK5R2 (involved in neuronal projection morphogenesis) (Ouyang et al. 2020) (Figure 5D).

To validate the findings from the ChIP-seq and GO analyses, we measured the mRNA levels of these genes in MCF-7 cells following treatment with each individual EDC (Figure 5E). The mRNA expression patterns aligned with the trends identified through the genomic analyses, confirming consistent upregulation or downregulation of the implicated genes. Collectively, these results provide valuable insights into the mechanisms of EDC-induced endocrine disruption and highlight the potential of certain pathways and genes as biomarkers for estrogenic compounds that act through EREs. Utilizing these biomarkers may significantly enhance the detection and evaluation of EDCs.

Discussion

The widespread presence of EDCs in everyday life underscores the urgent need for improved detection methods that not only extend beyond current OECD test guidelines but also illuminate the relationships between EDC binding–dimerization (Figure 1A, Undeveloped Issue 1) and dimerization–gene expression (Figure 1A, Undeveloped Issue 2). While existing protocols adequately address ligand binding and transcriptional activation, the intermediate steps linking these phases remain underexplored (Bolt et al. 2021). In this study, we aimed to fill these knowledge gaps by examining EDC binding affinities, evaluating their impact on ER dimerization, and correlating these findings with subsequent changes in gene expression – thus providing a more comprehensive perspective on EDC action (Matsushima et al. 2007).

Our DLS results demonstrated that ER dimerization can occur even in the absence of a bound ligand, with E2 stabilizing this dimeric state and simplifying it into a single, distinct species. This indicates that the receptor possesses an intrinsic capacity for dimerization, which is reinforced by ligand binding, potentially influencing receptor conformation, nuclear localization, and subsequent transcriptional events (Fuentes and Silveyra 2019). When comparing DLS and BRET experiments, the impact of non-ligand dimerization on the results from the same concentration of E2 treatment differs for each experiment. Although the same concentration of E2 is used, there are experimental variations: DLS measures particle size over a short time frame, while BRET assesses fluorescence after 24 hours of treatment. In the DLS results, all ER form dimers, so the peak BRET value should be reflective, but it appears this is not the case, likely due to the differing environments or processing times of the two experiments. Complementing these findings, ITC and BRET assays revealed a general correlation between EDC binding affinities and BRET ratios (Supplementary Table 3). While binding assays such as TG 493 focus on measuring ERα binding affinity, our BRET system provides the significant advantage of directly quantifying ER dimerization, and is applicable to both ERα and ERβ. ERβ can form heterodimers or homodimers with ERα, with differences in their tissue and cell expression profiles compared to ERα. This means that assays measuring dimerization can effectively assess estrogenic disruption across various tissues in the body. Furthermore, the BRET system can elucidate mechanistic details for EDCs showing discrepancies between binding affinity (assessed via TG 493) and ERE-mediated transactivation (assessed via TG 455). Such discrepancies underscore the importance of experimental conditions – such as EDC concentration – and the inherent limitations of ITC in capturing the transient states crucial for functional dimerization. While ITC provides valuable thermodynamic insights, the BRET assay (Choi et al. 2024), conducted in a live-cell context, is more sensitive to conformational transitions (Freyer and Lewis 2008). Together, these observations emphasize the need for multiple, complementary techniques to fully characterize EDC-receptor interactions.

The integrated approach used in this study, which combines DLS, ITC, BRET, and ChIP-seq analyses, enabled us to observe consistent trends among EDC binding, ER dimerization, and changes in gene expression (Shanle and Xu 2011). However, the differences in sensitivity and specificity among these

methods underscore the importance of carefully calibrating experimental parameters and considering physiologically relevant conditions (Teeguarden and Hanson-Drury 2013). Moreover, incorporating additional measurements – such as receptor-coregulator interactions, dimerization kinetics, and receptor conformational states – could further refine our understanding of how EDCs influence endocrine signaling (Matsushima et al. 2007).

Our use of non-cytotoxic EDC concentrations (1 μM) revealed subtle yet meaningful changes in gene expression. These minor shifts suggest that even low-dose, long-term exposure may result in cumulative endocrine effects, highlighting the importance of considering chronic, low-level exposures in risk assessment frameworks. This aligns with increasing evidence for non-monotonic dose–response relationships, which necessitate a reevaluation of current testing standards to better account for realistic exposure scenarios (Zoeller and Vandenberg 2015).

A key strength of our approach is the inclusion of both ERα and ERβ subtypes, which highlights the significant role of ER heterodimerization – an aspect often overlooked in conventional OECD guidelines that focus solely on ERα (OECD TG 455, OECD TG 493). Our findings indicate that ERβ and α/β heterodimers play substantial roles in shaping the downstream transcriptional landscape. This broader perspective on receptor diversity supports the incorporation of heterodimerization assays in standardized testing, potentially enhancing predictive accuracy for EDC risk assessment. Moreover, our ChIP-seq and GO analyses linked altered dimerization states to distinct biological pathways involved in immunity, cardiac induction, and hepatocyte growth factor signaling. These systems-level insights provide a clearer understanding of how EDCs disrupt complex regulatory networks and suggest new biomarkers or intervention strategies for mitigating EDC-induced health risks.

In conclusion, our study underscores the value of the BRET assay as a robust, standalone technique for detecting EDC activity while deepening our mechanistic understanding of how EDCs disrupt endocrine signaling. By addressing (Figure 1A, Undeveloped Issue 1) and (Figure 1A, Undeveloped Issue 2) – the binding–dimerization and dimerization–gene expression gaps – our work adds critical knowledge that complements existing guidelines and establishes a stronger foundation for EDC detection and characterization. This integrated approach can be extended to other nuclear receptors and signaling pathways, potentially enhancing the predictive power of EDC screening programs. As the global burden of EDCs continues to rise, such comprehensive and mechanistically informed strategies are increasingly essential for ensuring effective detection, regulation, and ultimately, the protection of public health.

Author contributions

Conceptualization: S.Y., H.L., and B.Y. Methodology: S.Y. and H.L. Validation: Y.-K.K. and G.L. Formal analysis: S.Y., H.L., and H.Y. Investigation: S.Y., H.L., Y.-K.K., and G.L. Resources: Y.-K.K., G.L., and H.-Y.L. Writing – original draft: S.Y. and H.L. Writing – review and editing: S.Y., H.Y., and B.Y. Visualization: S.Y. and H.L. Supervision: H.Y. and B.Y. Project administration: H.-Y.L. and B.Y. Funding acquisition: B.Y.

Disclosure statement

No potential conflict of interest was reported by the author(s).

Data availability statement

ChIP-seq raw data have been deposited in the GEO database (GSE291416). All data are available upon request on the corresponding authors.

References

Antony S, Antony S, Rebello S, George S, Biju DT RR, Madhavan A, Binod P, Pandey A, Sindhu R, et al. 2022. Bioremediation of endocrine disrupting chemicals- advancements and challenges. Environ Res. 213:113509. doi:10.1016/j.envres.2022.113509.

Bolt MJ, Singh P, Obkirchner CE, Powell RT, Mancini MG, Szafran AT, Stossi F, Mancini MA. 2021. Endocrine disrupting chemicals differentially alter intranuclear dynamics and transcriptional activation of estrogen receptor-α. iScience. 24:103227. doi:10.1016/j.isci.2021.103227.

Cheng M, Michalski S, Kommagani R. 2018. Role for Growth Regulation by Estrogen in Breast Cancer 1 (GREB1) in hormone-dependent cancers. Int J Mol Sci. 19(9):2543.

Choi G, Kang H, Suh JS, Lee H, Han K, Yoo G, Jo H, Shin YM, Kim TJ, Youn B. 2024. Novel estrogen receptor dimerization BRET-based biosensors for screening estrogenic endocrine-disrupting chemicals. Biomater Res. 28:0010. doi:10.34133/bmr.0010.

Diamanti-Kandarakis E, Bourguignon JP, Giudice LC, Hauser R, Prins GS, Soto AM, Zoeller RT, Gore AC. 2009. Endocrine-disrupting chemicals: an endocrine society scientific statement. Endocr Rev. 30:293–342. doi:10.1210/er.2009-0002.

Dutta S, Banu SK, Arosh JA. 2023. Endocrine disruptors and endometriosis. Reprod Toxicol. 115:56–73. doi:10.1016/j.reprotox.2022.11.007.

Freyer MW, Lewis EA. 2008. Isothermal titration calorimetry: experimental design, data analysis, and probing macromolecule/ligand binding and kinetic interactions. Methods Cell Biol. 84:79–113. doi:10.1016/S0091-679X(07)84004-0.

Fuentes N, Silveyra P. 2019. Estrogen receptor signaling mechanisms. Adv Protein Chem Struct Biol. 116:135–170. doi:10.1016/bs.apcsb.2019.01.001.

Gast K, Fiedler C. 2012. Dynamic and static light scattering of intrinsically disordered proteins. Methods Mol Biol. 896:137–161. doi:10.1007/978-1-4614-3704-8_9.

Han K, Suh JS, Choi G, Jang YK, Ahn S, Lee Y, Kim TJ. 2024. Novel FRET-based biosensors for real-time monitoring of estrogen receptor dimerization and translocation dynamics in living cells. Adv Sci (Weinh). 12:e2406907. doi:10.1002/advs.202406907.

Herrera FE, Garay AS, Rodrigues DE. 2014. Structural properties of CHAPS micelles, studied by molecular dynamics simulations. J Phys Chem B. 118:3912–3921. doi:10.1021/jp501729s.

Higuchi T, Orita T, Katsuya K, Yamasaki Y, Akiyama K, Li H, Yamamoto T, Saito Y, Nakamura M. 2004. MUC20 suppresses the hepatocyte growth factor-induced Grb2-Ras pathway by binding to a multifunctional docking site of met. Mol Cell Biol. 24:7456–7468. doi:10.1128/MCB.24.17.7456-7468.2004.

Huang RG, Li XB, Wang YY, Wu H, Li KD, Jin X, Du YJ, Wang H, Qian FY, Li BZ. 2023. Endocrine-disrupting chemicals and autoimmune diseases. Environ Res. 231:116222. doi:10.1016/j.envres.2023.116222.

ICCVAM. 2003. <Evaluation of in vitro test methods for detecting potential endocrine disruptors estrogen receptor and androgen receptor binding and transcriptional activation assays.pdf>.

Kim TS, Kim CY, Lee HK, Kang IH, Kim MG, Jung KK, Kwon YK, Nam HS, Hong SK, Kim HS, et al. 2011. Estrogenic activity of persistent organic pollutants and parabens based on the stably transfected human estrogen receptor-α transcriptional activation assay (OECD TG 455). Toxicol Res. 27:181–184. doi:10.5487/TR.2011.27.3.181.

Leclercq G, Gallo D, Cossy J, Laïos I, Larsimont D, Laurent G, Jacquot Y. 2011. Peptides targeting estrogen receptor alpha-potential applications for breast cancer treatment. Curr Pharm Des. 17:2632–2653. doi:10.2174/138161211797416048.

Liang J, Shang Y. 2013. Estrogen and cancer. Annu Rev Physiol. 75:225–240. doi:10.1146/annurev-physiol-030212-183708.

Marie C, Pierre A, Mayeur A, Giton F, Corre R, Grynberg M, Cohen-Tannoudji J, Guigon C J, Chauvin S. 2023-11-24. Dysfunction of human estrogen signaling as a novel molecular signature of polycystic ovary syndrome. Int J Mol Sci. 24(23):16689.

Matsushima A, Kakuta Y, Teramoto T, Koshiba T, Liu X, Okada H, Tokunaga T, Kawabata S, Kimura M, Shimohigashi Y. 2007. Structural evidence for endocrine disruptor bisphenol A binding to human nuclear receptor ERR gamma. J Biochem. 142:517–524. doi:10.1093/jb/mvm158.

Min J, Nwachukwu JC, Min CK, Njeri JW, Srinivasan S, Rangarajan ES, Nettles CC, Sanabria Guillen V, Ziegler Y, Yan S, et al. 2021. Dual-mechanism estrogen receptor inhibitors. Proc Natl Acad Sci U S A. 118(35):e2101657118.

Moon HJ, Shin HS, Lee SH, Hong EJ, Ahn C, Yoo YM, Jeung EB, Lee GS, An BS, Jung EM. 2023. Effects of prenatal bisphenol S and bisphenol F exposure on behavior of offspring mice. Anim Cells Syst (Seoul). 27:260–271. doi:10.1080/19768354.2023.2264905.

Nadeau M, Georges RO, Laforest B, Yamak A, Lefebvre C, Beauregard J, Paradis P, Bruneau BG, Andelfinger G, Nemer M. 2010. An endocardial pathway involving Tbx5, Gata4, and Nos3 required for atrial septum formation. Proc Natl Acad Sci U S A. 107:19356–19361. doi:10.1073/pnas.0914888107.

Nakato R, Sakata T. 2021. Methods for ChIP-seq analysis: a practical workflow and advanced applications. Methods. 187:44–53. doi:10.1016/j.ymeth.2020.03.005.

OECD. TG 455. OECD. 2021. Test No. 455: performance-based test guideline for stably transfected transactivation in vitro assays to detect estrogen receptor agonists and antagonists, OECD guidelines for the testing of chemicals, section 4, OECD Publishing, Paris.

OECD. TG 493. OECD, TG493. 2024. Test No. 493: performance-based test guideline for human recombinant estrogen receptor (hrER) in vitro assays to detect chemicals with ER binding affinity, OECD guidelines for the testing of chemicals, section 4, OECD Publishing, Paris.

Ouyang L, Chen Y, Wang Y, Chen Y, Fu AKY, Fu WY, Ip NY. 2020. p39-associated Cdk5 activity regulates dendritic morphogenesis. Sci Rep. 10:18746. doi:10.1038/s41598-020-75264-6.

Park J, Lee H, Kweon J, Park S, Ham J, Bazer FW, Song G. 2024. Mechanisms of female reproductive toxicity in pigs induced by exposure to environmental pollutants. Mol Cells. 47:100065. doi:10.1016/j.mocell.2024.100065.

Park Y, Jang MJ, Ryu DY, Lim B, Pathak RK, Pang MG, Kim JM. 2024. Integrative transcriptomic profiling uncovers immune and functional responses to bisphenol a across multiple tissues in male mice. Anim Cells Syst (Seoul). 28:519–535. doi:10.1080/19768354.2024.2419473.

Perkins MS, Louw-du Toit R, Jackson H, Simons M, Africander D. 2022. Upregulation of an estrogen receptor-regulated gene by first generation progestins requires both the progesterone receptor and estrogen receptor alpha. Front Endocrinol (Lausanne). 13:959396.

Rachoń D. 2015. Endocrine disrupting chemicals (EDCs) and female cancer: informing the patients. Rev Endocr Metab Disord. 16:359–364. doi:10.1007/s11154-016-9332-9.

Rölle A, Meyer M, Calderazzo S, Jäger D, Momburg F. 2018. Distinct HLA-E peptide complexes modify antibody-driven effector functions of adaptive NK cells. Cell Rep. 24:1967–1976.e1964. doi:10.1016/j.celrep.2018.07.069.

Shanle EK, Xu W. 2011. Endocrine disrupting chemicals targeting estrogen receptor signaling: identification and mechanisms of action. Chem Res Toxicol. 24:6–19. doi:10.1021/tx100231n.

Sorsby M, Almardini S, Alayyat A, Hughes A, Venkat S, Rahman M, Baker J, Rana R, Rosen V, Liu ES. 2024. The role of GDF5 in regulating enthesopathy development in the Hyp mouse model of XLH. J Bone Miner Res. 39:1162–1173.

Souza DS, Lombardi APG, Vicente CM, Lucas TFG, Erustes AG, Pereira GJS, Porto CS. 2019. Estrogen receptors localization and signaling pathways in DU-145 human prostate cancer

cells. Mol Cell Endocrinol. 483:11–23. doi:10.1016/j.mce.2018.12.015.

Tamrazi A, Carlson KE, Daniels JR, Hurth KM, Katzenellenbogen JA. 2002. Estrogen receptor dimerization: ligand binding regulates dimer affinity and dimer dissociation rate. Mol Endocrinol. 16:2706–2719. doi:10.1210/me.2002-0250.

Teeguarden JG, Hanson-Drury S. 2013. A systematic review of bisphenol A "low dose" studies in the context of human exposure: a case for establishing standards for reporting "low-dose" effects of chemicals. Food Chem Toxicol. 62:935–948. doi:10.1016/j.fct.2013.07.007.

Welboren WJ, Sweep FC, Span PN, Stunnenberg HG. 2009. Genomic actions of estrogen receptor alpha: what are the targets and how are they regulated? Endocr Relat Cancer. 16:1073–1089. doi:10.1677/ERC-09-0086.

Yilmaz B, Terekeci H, Sandal S, Kelestimur F. 2020. Endocrine disrupting chemicals: exposure, effects on human health, mechanism of action, models for testing and strategies for prevention. Rev Endocr Metab Disord. 21:127–147. doi:10.1007/s11154-019-09521-z.

Yoon K, Kwack SJ, Kim HS, Lee BM. 2014. Estrogenic endocrine-disrupting chemicals: molecular mechanisms of actions on putative human diseases. J Toxicol Environ Health B Crit Rev. 17:127–174. doi:10.1080/10937404.2014.882194.

Zacharia LC. 2017. Permitted daily exposure of the androgen receptor antagonist flutamide. Toxicol Sci. 159:279–289. doi:10.1093/toxsci/kfx135.

Zoeller RT, Brown TR, Doan LL, Gore AC, Skakkebaek NE, Soto AM, Woodruff TJ, Vom Saal FS. 2012. Endocrine-disrupting chemicals and public health protection: a statement of principles from the endocrine society. Endocrinology. 153:4097–4110. doi:10.1210/en.2012-1422.

Zoeller RT, Vandenberg LN. 2015. Assessing dose-response relationships for endocrine disrupting chemicals (EDCs): a focus on non-monotonicity. Environ Health. 14:42. doi:10.1186/s12940-015-0029-4.